Rapid Transport of Water via a Carbon Nanotube Syringe

Jose L. Rivera[†,‡] and Francis W. Starr*[,†]

Department of Physics, Wesleyan University, Middletown, Connecticut 06457, and Instituto de Investigaciones en Materiales, Universidad Nacional Autónoma de México, Apartado Postal 70-360, 04510 México DF, México

Received: July 10, 2009; Revised Manuscript Received: January 15, 2010

The controlled flow of water molecules at the nanoscale is an initial step to many fluidic processes in nanotechnology. Here we show how thin films of water can be drawn through a nanosyringe built from a carbon nanotube membrane and a "plunger". By increasing the speed of withdrawal of the plunger, we can obtain molecular transport through the membrane at flux rates exceeding 10^{25} molecules cm^{-2} s^{-1}. Above a threshold speed around 0.25 nm/ns (25 cm/s), molecules cannot fill the chamber created by the plunger motion as fast as the chamber expands, and the resulting flux rate drops. By considering hydrophobic or hydrophilic plungers, we unexpectedly find that the nature of the water-plunger interactions does not affect the flux rate or the threshold plunger speed. While the water structure near the plunger surface differs significantly for different plunger interactions, the failure of the film away from the plunger surface is responsible for loss of transport. As a result, the surface interactions play a limited role in controlling the flux.

1. Introduction

The control of water transport using nanostructures is important for a vast array of technologies,[1] including drug delivery, fluid separation, and biological channels. Defect-free carbon structures are particularly promising for transport, since water can form a structured hydrogen-bond network inside nanopores[2–5] that has only weak attraction to the carbon nanostructures,[6,7] resulting in a large molecular flux with low flow friction.[8–10] The large fluxes have been attributed to the smoothness of the nanotube walls.[9] Carbon nanotube membranes (CNM) (with nanotube diameters between 1.3−2[11] and 3.5 nm[12]) have been experimentally studied, and these materials achieved large mass transport fluxes by differences in chemical potential, pressure, or temperature to drive the flow of water across the membranes. Additionally, small deformations do not significantly affect flux, but any deformation beyond a critical amount will cause a reduction of flux.[13] Alternatively, mobile charges located outside the carbon nanotubes can induce an ordering of the water molecules along the nanotube channel facilitating the flow of water molecules; this can increase the magnitude of the flow by a factor 20.[14–16] Simulations of water transport through CNM driven by osmotic forces have shown high flow rates (5.8 water molecules per ns for each nanotube).[17]

In this work, we examine a complementary approach, in which molecules are drawn across a membrane, rather than forced through tubes by pressure-induced flows. Specifically, we examine the possibility of controlling the flow of water through a nano-"syringe" consisting of a CNM and a surface acting as a plunger. In this approach, one expects the driving force is a vacuum effect provided by the nanosyringe, rather than the applied pressure. We find that we can achieve flux values as large or larger than those obtained via pressure driven flows.[14,17] Surprisingly, our results are independent of the water-plunger interactions, suggesting that the packing of molecules in a narrow film plays a more important role.

* To whom correspondence should be addressed. E-mail: joserivera@iim.unam.mx (J.L.R.); fstarr@wesleyan.edu (F.W.S.).
† Wesleyan University.
‡ Universidad Nacional Autónoma de México.

The paper is arranged as follows: In section 2 we described the membrane and nanosyringe molecular models and the methodology employed in this work. Section 3 contains the results for the simulations of water flow through carbon nanotube membranes and the flow control using nanosyringes with hydrophilic and hydrophobic plungers. The conclusions of this work are presented in section 4.

2. Models and Computational Protocol

The membrane we study consists of two graphene sheets connected by a (6,6) carbon nanotube. This choice of the nanotube chirality makes it possible to form a continuous and smooth surface junction between the end of the nanotube and the graphene sheet (Figure 1a). The nanotube length is 1.96 nm; the effective radius of the nanotube is 0.244 nm (after subtracting the atomic core exclusion size), resulting in an effective cross-sectional area of 0.187 nm^2 for the transport of water molecules. The syringe plunger consists of either a hydrophobic graphene sheet (Figure 1b) or a hydrophilic hydroxylated silica (HS) surface (Figure 1e) at one side of the nanotube. We use periodic boundary conditions in the directions perpendicular to the nanotube, so the system may be considered a membrane of regularly ordered nanotubes. For the graphene plunger, the sheet has dimensions 2.13 × 1.97 nm, resulting in a density $n = 0.2381$ nm^{-2} of nanotubes in the periodic array. The HS plunger has dimensions 2.58 × 1.97 nm, yielding $n = 0.1968$ nm^{-2}. The density in this case is slightly smaller than the density of the hydrophobic system because the HS molecular structure dictates that the size nearest to that of the graphene membrane that can be simulated using periodic conditions is slightly larger than the graphene membrane. We carry out all molecular dynamics simulations at ambient temperature 298.15 K.

We use the molecular dynamics methodology[18] to simulate the flow of water molecules through nanosyringes using carbon nanotube membranes. We integrate the equations of motion using the Gear fourth-order predictor-corrector algorithm with a time step of 1 fs and control the temperature using the Gaussian isokinetic thermostat[19,20] and the Evans−Murad qua-

10.1021/jp906527c
Published on Web 02/12/2010

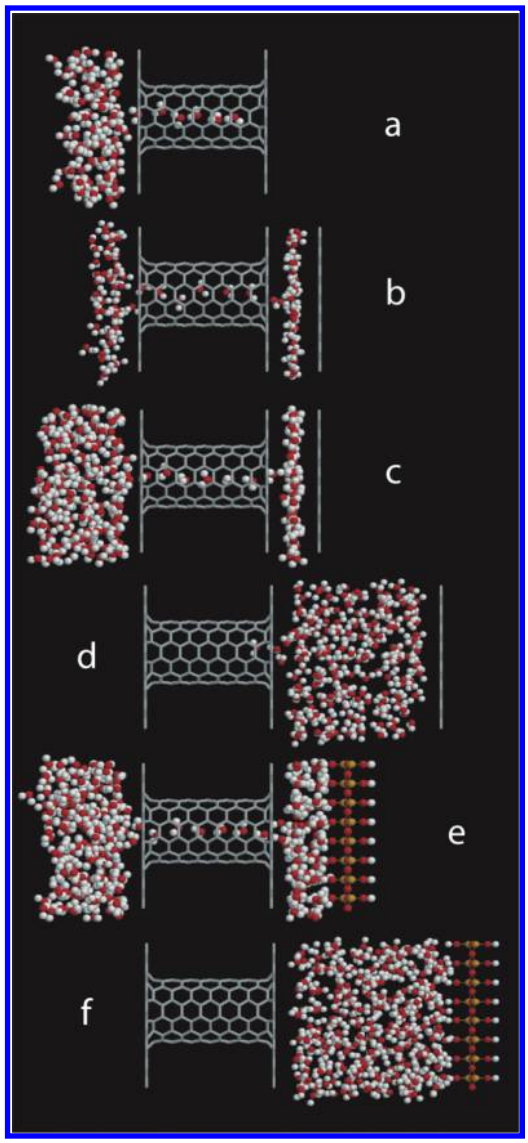

Figure 1. Snapshots of water flow through the nanosyringe. (a) Thin film of water after wetting and penetrating the CNM. (b) Flow of water molecules into the chamber of the nanosyringe with the plunger located at 0.68 nm from the membrane. (c) The addition of water molecules outside the free space of the CNM causes the number of water molecules inside the chamber to increase slightly. (d) After moving the graphene wall at $v_w = 0.25$ nm/ns, all water molecules are transferred into the chamber after 5.2 ns. (e) Water also flows inside the chamber when a hydrophilic wall made of HS is placed at 0.68 nm, forming two layers of water. (f) After moving the HS wall at $v_w = 0.25$ nm/ns, all water molecules are transferred into the chamber after 4.9 ns.

ternion formalism.[21] We prefer to simulate the system at constant temperature rather than constant energy, since the nanostructures that form the nanosyringes are rigid, and they dissipate heat and momentum as in real systems.

We employ the TIP5P force field to simulate water molecules, which uses spherical cutoffs for Lennard-Jones and Coulombic interactions (9 Å).[22] Carbon atoms in the carbon nanotube membrane and the graphene wall are rigid in our simulations, and the Lennard-Jones parameters have been used to predict successfully the packing structures in graphite and fullerenes C_{60} and C_{70}.[23] We simulate the water−nanotube and water−graphene interactions using the Lorentz−Berthelot mixing rules. The water−carbon interactions play an important role in the water filling and flow through CNM,[7] and the correct potential for the interactions is not known. If we decrease the strength of the water−carbon interaction, the capacity of water molecules to fill and flow through the CNM decreases. There are other phenomena that may also play an important role in the water transport. For example, carbon atoms near the end of the nanotube, forming the junction with the graphene sheet are generally more stressed than carbon atoms near the axial center of the nanotubes, and have stronger interactions with the water molecules.[6,24] Electric fields produces polarization effects on the carbon atoms and water molecules, affecting both ways the filling and flow processes.[24–27] These are important issues to consider as the potential models become more sophisticated and computationally tractable.

Atoms in the hydroxylated silica wall are also rigid and interact with water molecules through Coulombic and Lennard-Jones oxygen (silica)−oxygen (water) interactions.[28,29] We simulate rigid nanostructures (carbon nanotube membrane and plunger walls) to speed up the long runs of simulations (∼70 ns) needed in the studied phenomena. We restrict the movement of the atoms in the graphene and HS walls to only displace in the axial direction at constant velocity to mimic the plunger movement in the syringe effect.

The initial conformation of water molecules (25 molecules) consists of a cubic cell near one end and outside the carbon nanotube membrane. We obtain the initial conformation of a wider system by reproducing the initial conformation of the system (25 molecules) along the axis parallel to the carbon nanotube. The cubic cell is periodic in 2 dimensions along the perpendicular direction to the carbon nanotube. We consider systems with 25−275 water molecules. Once some of the molecules flow to the chamber of the nanosyringe, we add water molecules outside the carbon nanotube membrane to simulate wider systems.

3. Results

Before we attempt draw water through the nanotube using a nano syringe, we first simulate thin water films of increasing width near the CNM without a plunger surface to check if some molecules spontaneously flow trough the CNM, which will be important for starting the syringe. Although carbon is traditionally considered hydrophobic, the water films wet the CNM surface near the nanotube and spontaneously penetrate the CNM (Figure 1a). The amount of nanotube filling depends on the thickness of the water film. For film widths up to one complete monolayer of water molecules, the channel of the CNM fills completely with water and remains filled over an entire simulation (50 ns). In these extremely thin films, the network of hydrogen bonds is not fully developed, which facilitates the penetration of water molecules into the CNM. As we increase the width of the film outside the CNM, water molecules intermittently penetrate and retract from the nanotube interior. The duration of time that molecules spend in the tube is nearly independent of the film thickness; the interval between successive fillings grows as the thickness increases. In these thicker films, the network of hydrogen bonds is more developed, making it more difficult for a small number of molecules to separate from the film and penetrate the nanotube, consistent with the increased intermittency of the filling. This intermittency indicates that thermal fluctuations play a significant role. In other words, thermal fluctuations enable the penetration of water molecules into the CNM, but the stronger network of hydrogen bonds pulls molecules back to the film, preventing a permanent filling. As a result, it will be extremely rare for thermal fluctuations to transfer all water molecules to the other side of the CNM for

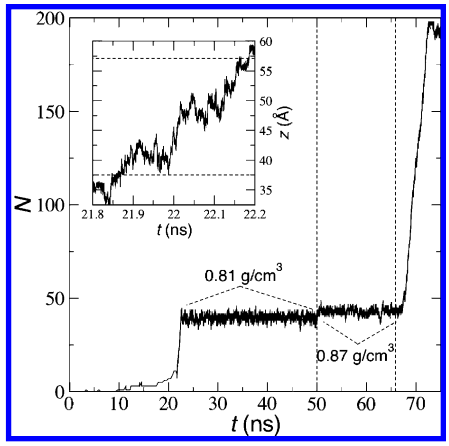

Figure 2. Nanotube filling and syringe behavior, measured by the number of molecules N in the chamber as a function of time. From 0 to 50 ns, the water molecules from a bilayer film in the free space outside the CNM flow spontaneously into the chamber of the nanosyringe. At 50 ns, we increase the number of molecules in the water film in the free space outside the CNM, resulting in an increase of N inside the chamber. At 65.8 ns the graphene wall starts to move at $v_w = 0.25$ nm/ns, causing the flow of additional molecules into the chamber of the nanosyringe, until all the water molecules move into the chamber. Numbers in parentheses represent the standard deviation of the densities. Inset graph: Profile of the intermittent motion of one water molecule moving across the CNM as a function of time. Dotted lines represent the end positions of the nanotube.

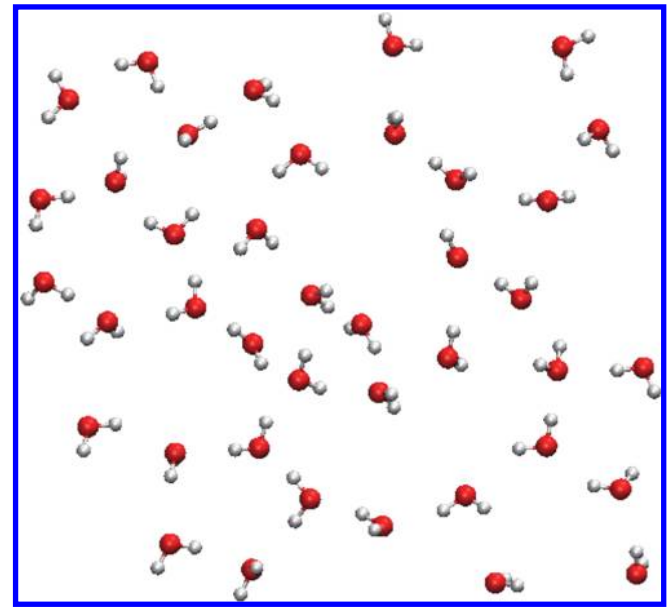

Figure 3. Snapshot of the front view of water molecules inside the chamber of the nanosyringe. The chamber contains 44 molecules and the conformation represents a state when the chamber is filled (>25 ns in Figure 2) but before adding more molecules outside the CNM (<50 ns in Figure 2).

thicker films. Indeed, we did not observe any water molecules that flow to the opposite side of the membrane. Accordingly, some driving force is required to cause molecules to flow through the tube, which can be provided by the plunger of our syringe.

We promote the flow of water molecules to the other side of the CNM by placing a graphene wall on the initially unfilled side of the CNM. The graphene sheet is parallel to the CNM at a fixed distance of 0.68 nm (Figure 1b). This width is just large enough to accommodate a single monolayer of water molecules. Although graphene is normally considered hydrophobic, water molecules move into the chamber due to the van der Waals attractions.

With the graphene sheet in place, molecules from the monolayer of water on the free side of the membrane begin to traverse the nanotube and fill the plunger chamber after roughly 10 ns (Figure 2). The molecules form a monolayer inside the chamber with a density of $\rho_c = 0.81$ g/cm^3 (with standard deviation 0.03 g/cm^3). Most of the water molecules in this monolayer are oriented parallel to the graphene surface (Figure 3), forming a weak bond network. We calculate the density using the free van der Waals space inside the chamber (which takes into account that the surface atoms occupy a finite volume determined from their van der Waals radii). At ≈21.8 ns, with 11 or 12 water molecules inside the chamber, the flow of molecules increases dramatically (Figure 2); Figure 1b shows pictorially the filling at this stage. The filling proceeds at a nearly constant flux of 22.52×10^{24} molecules cm^{-2} s^{-1} (Figure 2 inset). Curiously, this flux value is several orders of magnitude larger than that reported for experiments using CNM with wider nanotubes with external driving flow pressure.[11,12] However, Thomas and McGaughey showed that the flow rate has an inverse dependence with the nanotube diameter for systems under external pressure.[10] Thus the observation of a larger flux for our system than that of wider nanotubes is not surprising. Additionally, the flux we observe is of the same order of magnitude found in simulations of pressure-driven water flow through similar diameter nanotubes at the same temperature.[30]

Water molecules flow through the CNM forming a single-file water chain,[16] and due to the small diameter of the nanotube, no water molecules flow in the opposite direction during the computation of the fluxes. Therefore, the flux values we report in this work also represent the net flux values. Compared to simulations of flow driven by osmotic forces,[17] the net flux values for the spontaneous filling of the chamber in this work are 7 times higher than the spontaneous process driven by osmotic forces, suggesting that the vacuum inside the chamber provides a larger driving force than the osmotic forces. The flow of individual water molecules is not ballistic; instead the transfer of a water molecule through the CNM occurs by a sequence of small forward and backward movements (Figure 2 inset). An animation of this process can be seen in the Supporting Information, and suggests that some type of correlated random walk might be appropriate to describe the motion. Considering all molecules that traverse the tube, we find net speeds ranging from 4 to 22 nm/ns.

We also test the behavior of thicker films, which only intermittently fill the tube in the absence of the graphene sheet. Over the period of 50 ns of simulation time, we find that for films with widths up to 3 monolayers, water molecules will flow across the CNM into the chamber. For thicker films with a well-developed hydrogen bond network, we do not observe filling of the chamber over the same period of time; simulations over a longer duration may also eventually show filling of the chamber for thick films. To accelerate the filling of these thick films, we can start from a thin film where the chamber is already filled spontaneously, and add more molecules to the open side of the CNM. One might expect the water−water attractions to pull molecules from the filled chamber, but when we add additional water molecules on the free side, the number of water molecules inside the chamber actually slightly increases (Figure 1c). Figure 2 reflects this change as a small increase in the number of molecules inside the chamber at 50 ns, which also slightly increases the density of the monolayer inside the chamber (Figure 1c). As we add more water molecules on the free side of the CNM, we find that the density of the monolayer

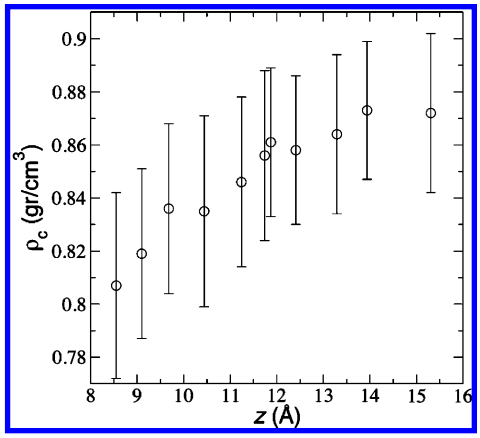

Figure 4. Chamber density ρ_c as a function of the width of the water thin film in the free space outside the carbon-nanotube membrane. The error bars represent the standard deviations of the values.

inside the chamber grows to an asymptotic value $\rho_c = 0.87$ g/cm^3 (Figure 4).

Since molecules are attracted to the graphene chamber, we should be able to "pull" molecules through the CNM by moving the wall, creating our nanosyringe. We start the simulation from a configuration with a filled chamber (Figure 1c). For simplicity, we move the wall at a constant velocity v_w. Figure 2 shows an example where we move the graphene wall at fixed $v_w = 0.25$ nm/ns starting at 65.8 ns. This produces an immediate influx of the remaining water molecules from the water film on the free side of the CNM to the chamber, until the chamber fully fills (Figure 1d). At $v_w = 0.25$ nm/ns, the transfer of molecules occurs at an almost constant rate for ~5.2 ns, resulting in a nearly constant flux of 15.62×10^{24} molecules cm^{-2} s^{-1}. This result demonstrates the possibility to use a syringe-like effect to transfer water through the CNM. An animation of this process can also be seen in the Supporting Information. Since no water molecules flow in the opposite direction, the flux also represents the net flux. Compared to the simulations of a "nano-pump" driven by mobile external charges,[14] the net flux values for the nanosyringe are ~3 times higher than the maximum net flux achieved by the pump. The higher net fluxes are probably due to coherent effect of the plunger; specifically, the plunger directly pulls water molecules inside the CNM in the axial direction, while the mobile charges pull the molecules indirectly, generating forces in the both the axial and radial directions.

Below some threshold of v_w, moving the wall results in the complete transfer of molecules across the CNM. Naturally, there must be some maximal rate at which molecules can be transferred across the CNM. Accordingly, we examine a range of values for v_w to find the limiting flux across the CNM. In this case, we calculate the mean flux J from the time needed for all molecules not initially in the chamber to traverse the CNM; we show the dependence of J on v_w in Figure 5a. For $v_w \leq 0.25$ nm/ns, we observe the formation of a homogeneous liquid in the chamber with a final density $\rho_c = 0.78$ gr/cm^3. While the surface is being moved, the transient value of ρ_c can be as low as 0.6 gr/cm^3 (Figure 6). For values of $v_w > 0.25$ nm/ns, the graphene wall separates from the liquid in the chamber after 2 ns, resulting in a large cavity. Due to the initial impulse that the graphene wall provides to the liquid, the liquid continues flowing and completely passes through the CNM. However, the break of the fluid results in a flux that is significantly smaller than the maximum flux we obtain at $v_w = 0.25$ nm/ns. At higher velocities, separation occurs more rapidly, and as a result, the wall does not provide enough impulse to the liquid for it to traverse the membrane; in some cases, the water may even flow back to the free side of the CNM. These results clearly indicate that there is a critical value for v_w for the maximal flux, above which reliable transfer of water will not occur. It is interesting to note that, once the water molecules penetrate the chamber, they generate a strong pressure on the plunger, on the order of GPa (Figure 7). In principle, this pressure could move the plunger by itself, allowing more water molecules to cross the CNM. Once all the water molecules flow through the CNM, the pressure in the plunger drops to zero, because the liquid inside the chamber remains near the end of the CNM.

Given the success with a hydrophobic surface, one might expect that the syringe will be more effective if we use a hydrophilic surface as plunger. Therefore, we also simulate the behavior of the nanosyringe mechanism using a wall made of HS (Figure 1e). We again use a separation of 0.68 nm between the centers of the carbon atoms in the inner wall of the CNM and the center of the hydrogen atoms of the HS to allow for an initial film of water to form before moving the surface. For this system, we also allow the chamber to prefill before moving the plunger, following the same protocol used for the graphene surface; similarly, water molecules will spontaneously fill the chamber for thin films. Although we use the same separation between the membrane and plunger used for the graphene wall system, the water molecules form two water layers inside the chamber due to strong attraction to the hydroxyl groups tethered to the silica (Figure 8). The water layer near the hydrophilic wall (HS) shows a smaller density because water molecules bind strongly to the hydroxyl end groups of the HS surface, and these OH groups have a larger separation (≈0.5 nm) than preferred by the water molecules. Accordingly, the molecules pack more densely away from the wall. Similar result were found in molecular simulations of liquid water near graphite and HS surfaces.[31]

To determine if molecules can be more rapidly transferred across the CNM with the hydrophilic surface, we test the dependence of J on v_w (Figure 5a). Curiously, the maximum v_w we can achieve using the HS wall without breaking the water film in the chamber is identical to the maximum v_w for the hydrophobic graphene wall. However, the hydrophilic system reaches larger fluxes than the hydrophobic system for the same v_w. At velocities above the threshold breaking speed, the water molecules do not continue flowing, or the molecules simply stop, and sometimes retract to the free side the CNM, just as in the graphene case.

Due to the different nanotube densities per unit area of CNM, we can make a more appropriate comparison by plotting the flux rates as a function of the rate of volume increase dV/dt inside the chamber as we move the wall at constant v_w (Figure 5b). Using dV/dt on the abscissa, the fluxes for both systems collapse to a master curve. Hence, both systems exhibit the same behavior; the apparent flux for HS in terms of the v_w is only due to the smaller density of carbon nanotubes per unit area of CNM. In other words, we find the unexpected result that the nature of the surface chemistry of the plunger plays no apparent role in the flux of water through the syringe.

In order to understand the independence of the flux results on the nature of the plunger, we analyze the structural properties of the initial layers formed inside the chamber. Figure 9 shows the radial distribution function (rdf) $g_{||}(r)$ in the plane of the wall for oxygen−oxygen water pairs. The rdf is the probability to find an oxygen atom at a distance, r, away from another oxygen atom, in the plane parallel to the CNM wall. For the

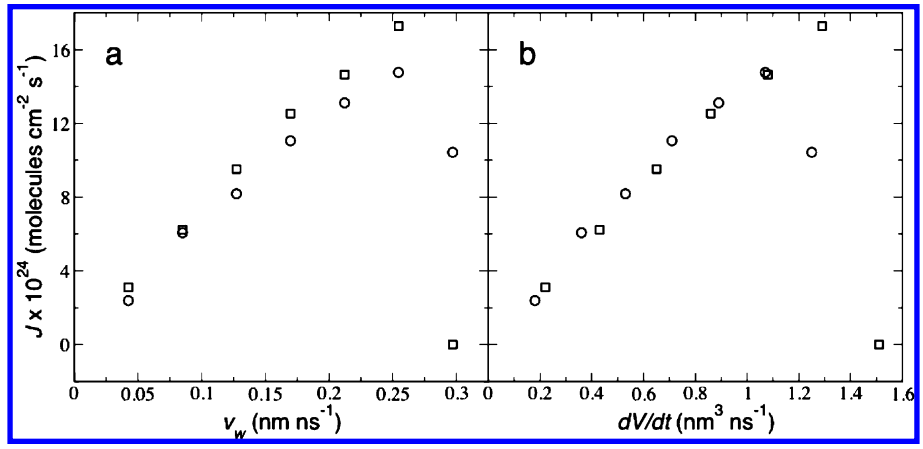

Figure 5. Flux of water molecules crossing the CNM as a function of (a) υ_w and (b) dV/dt, at 298.15 K. Circle and square symbols represent the results of the hydrophobic and hydrophilic plunger, respectively.

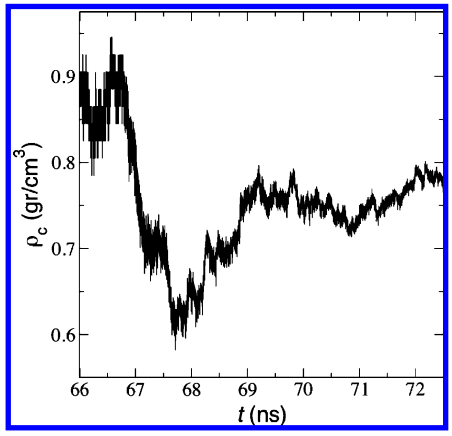

Figure 6. Chamber density ρ_c as a function of the simulation time. At 65.8 ns the graphene wall of the chamber starts moving at a constant lineal $\upsilon_w = 0.25$ nm/ns.

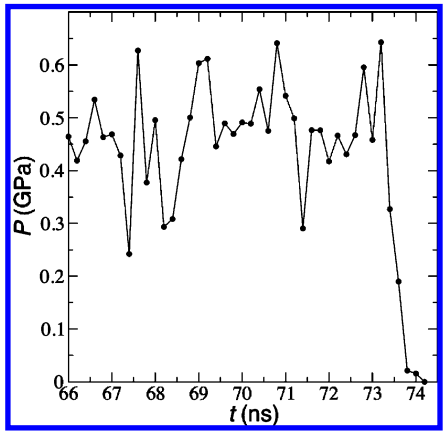

Figure 7. Plunger pressure, calculated from the normal component of the force, as a function of the time. At 65.8 ns the graphene wall of the chamber starts moving at a constant lineal $\upsilon_w = 0.25$ nm/ns.

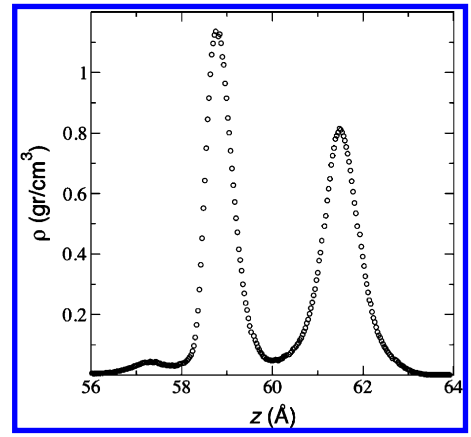

Figure 8. Density of water molecules as a function of the position inside the chamber. The hydrophilic wall is located on the far right. Two well-defined layers of water form inside the chamber before the plunger is moved.

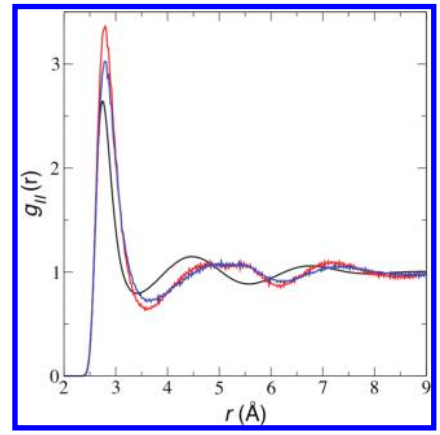

Figure 9. Radial distribution function $g_{ll}(r)$ as a function of the oxygen - oxygen separation, parallel to the CNM wall, at 298.15 K. Red and blue lines represent the systems with the graphene and HS walls, respectively. Black line represents bulk water at 298.15 K. Note that $g_{ll}(r)$ is nearly identical for both hydrophobic and hydrophilic surfaces.

system with the graphene wall, we calculate $g_{ll}(r)$ for the central 0.1 nm of the chamber; for the system with the HS wall, we calculate $g_{ll}(r)$ for the water layer nearest the CNM. Relative to $g_{ll}(r)$ for bulk liquid water, we find that the first neighbor peak increases in amplitude, while the second neighbor peak at 0.45 nm nearly shifts to near 0.5 nm. The change in the second neighbor peak location indicates the loss of tetrahedral order, which is not surprising given the confinement of the film. These structural changes are similar to those reported in the literature for a bilayer of water between graphene plates separated by 1.1 nm. In the bilayer system, the structural effects are less pronounced at the same density and temperature.[32,33] More significant is the fact that $g_{ll}(r)$ for the hydrophobic and hydrophilic walls are nearly identical, the only difference being that the hydrophilic system has a smaller first neighbor peak than that of the hydrophobic system. Accordingly, the first layer near the CNM in the hydrophilic system can be considered nearly the same as a monolayer between two hydrophobic walls.

Therefore, taking in consideration the structural similarity of the water in the chamber for the two systems, it is not surprising that the chemical composition of the plunger has a negligible effect on the flux results. In other words, the structure of the water in the chamber is dominated by packing constraints in the narrow region, rather than the surface interactions. As a result, the water−water interactions, which are the limiting factor for the breaking of homogeneous fluid in the syringe, are nearly the same for either type of plunger surface.

4. Conclusions

The controlled flow of water films using nanosyringes made of thin carbon nanotubes shows a promising future. The mechanism we investigated show the potential to move water films using plunger velocities up to about 0.25 nm/ns, giving rise to flux rates on the order of mol cm^{-2} s^{-1}. Most unexpected is the observation that the chemical composition of the plunger does not play a major role in the flux rates. This appears to be due to the packing constraints of the water in the narrow chamber. As a result the water−water interactions play a dominant role, rather than water-surface interactions. We also note that thin films of water molecules flow spontaneously into the chamber of the nanosyringe at fluxes higher than the fluxes obtained moving the hydrophobic or hydrophilic walls; this spontaneous flux appears to be an upper limit on the flux rates for the syringe. The feasibility of the nanosyringe device will depend on the control over the positioning of the plunger wall near the end of the carbon nanotube membrane. The advances in positioning devices for atomic force microscopy applications in the nanoscale should make such a device achievable. The nanosyringe device could find applications in processes that require precise control of the flow of fluids, such as micro- (MEMS) and nanoelectromechanical systems (NEMS), with specific applications in drug delivery, nano fluid separations, and dynamics.

Acknowledgment. We thank the U.S. Department of Energy and the National Science Foundation for support under Grant No. DMR-0427239. We also thank CONACYT (México) for support under Grant No. 48568. J.L.R. thanks Maria Carolina Dos Ramos and Guillermo Ibarra for a critical reading the manuscript.

Supporting Information Available: Movies showing the transport of water through a carbon nanotube syringe. This material is available free of charge via the Internet at http://pubs.acs.org.

References and Notes

(1) Whitby, M.; Quirke, N. *Nat. Nanotechnol.* **2007**, *2*, 87.
(2) Rasaiah, J. C.; Garde, S.; Hummer, G. *Annu. Rev. Phys. Chem.* **2008**, *59*, 713.
(3) Striolo, A. *Nanotechnology* **2007**, *18*, 10.
(4) Hanasaki, I.; Nakatani, A. *Nanotechnology* **2006**, *17*, 2794.
(5) Rivera, J. L.; McCabe, C.; Cummings, P. T. *Nano Lett.* **2002**, *2*, 1427.
(6) Rivera, J. L.; Rico, J. L.; Starr, F. W. *J. Phys. Chem. C* **2007**, *111*, 18899.
(7) Hummer, G.; Rasaiah, J. C.; Noworyta, J. P. *Nature* **2001**, *414*, 188.
(8) Sholl, D. S.; Johnson, J. K. *Science* **2006**, *312*, 1003.
(9) Joseph, S.; Aluru, N. R. *Nano Lett.* **2008**, *8*, 452.
(10) Thomas, J. A.; McGaughey, A. J. H. *Nano Lett.* **2008**, *8*, 2788.
(11) Holt, J. K.; Park, H. G.; Wang, Y. M.; Stadermann, M.; Artyukhin, A. B.; Grigoropoulos, C. P.; Noy, A.; Bakajin, O. *Science* **2006**, *312*, 1034.
(12) Majumder, M.; Chopra, N.; Andrews, R.; Hinds, B. J. *Nature* **2005**, *438*, 44.
(13) Wan, R. Z.; Li, J. Y.; Lu, H. J.; Fang, H. P. *J. Am. Chem. Soc.* **2005**, *127*, 7166.
(14) Gong, X. J.; Li, J. Y.; Lu, H. J.; Wan, R. Z.; Li, J. C.; Hu, J.; Fang, H. P. *Nat. Nanotechnol.* **2007**, *2*, 709.
(15) Li, J. Y.; Gong, X. J.; Lu, H. J.; Li, D.; Fang, H. P.; Zhou, R. H. *Proc. Natl. Acad. Sci. U.S.A.* **2007**, *104*, 3687.
(16) Fang, H. P.; Wan, R. Z.; Gong, X. J.; Lu, H. J.; Li, S. Y. *J. Phys. D-Appl. Phys.* **2008**, *41*, 16.
(17) Kalra, A.; Garde, S.; Hummer, G. *Proc. Natl. Acad. Sci. U.S.A.* **2003**, *100*, 10175.
(18) Frenkel, D.; Smit, B. *Understanding Molecular Simulation: From Algorithms to Applications*; Academic Press, Inc.: New York, 1996.
(19) Hoover, W. G.; Ladd, A. J. C.; Moran, B. *Phys. Rev. Lett.* **1982**, *48*, 1818.
(20) Evans, D. J.; Morriss, G. P. *Phys. Lett. A* **1983**, *98*, 433.
(21) Evans, D. J.; Murad, S. *Mol. Phys.* **1977**, *34*, 327.
(22) Mahoney, M. W.; Jorgensen, W. L. *J. Chem. Phys.* **2000**, *112*, 8910.
(23) Guo, Y. J.; Karasawa, N.; Goddard, W. A. *Nature* **1991**, *351*, 464.
(24) Zimmerli, U.; Gonnet, P. G.; Walther, J. H.; Koumoutsakos, P. *Nano Lett.* **2005**, *5*, 1017.
(25) Zhu, F. Q.; Schulten, K. *Biophys. J.* **2003**, *85*, 236.
(26) Vaitheeswaran, S.; Rasaiah, J. C.; Hummer, G. *J. Chem. Phys.* **2004**, *121*, 7955.
(27) Dzubiella, J.; Hansen, J. P. *J. Chem. Phys.* **2005**, *122*, 14.
(28) Giovambattista, N.; Rossky, P. J.; Debenedetti, P. G. *Phys. Rev. E* **2006**, *73*, 14.
(29) Raviv, U.; Laurat, P.; Klein, J. *Nature* **2001**, *413*, 51.
(30) Corry, B. *J. Phys. Chem. B* **2008**, *112*, 1427.
(31) Argyris, D.; Tummala, N. R.; Striolo, A.; Cole, D. R. *J. Phys. Chem. C* **2008**, *112*, 13587.
(32) Kumar, P.; Buldyrev, S. V.; Starr, F. W.; Giovambattista, N.; Stanley, H. E. *Phys. Rev. E* **2005**, *72*, 12.
(33) Kumar, P.; Starr, F. W.; Buldyrev, S. V.; Stanley, H. E. *Phys. Rev. E* **2007**, *75*, 8.

JP906527C